

Optimum Wing Sizing of a Single-Stage-to-Orbit Vehicle

Alan W. Wilhite*

NASA Langley Research Center, Hampton, Virginia

An investigation has been conducted to determine preliminary wing designs for a single-stage-to-orbit (SSTO) vehicle. This vehicle has the following mission profile: vertical takeoff, boost-to-orbit, hypersonic re-entry, and horizontal landing. For this vehicle, the wing is sized to meet Space Shuttle re-entry aerodynamic requirements for hypersonic trim and horizontal landing, since re-entry trajectories for the Shuttle and the SSTO vehicle are similar. A hypersonic and subsonic aerodynamic computer program was developed and combined with an existing optimization algorithm to automatically size and shape a wing that satisfies both re-entry and landing requirements while also maintaining a minimum mass design. With this procedure, the influence of hypersonic and subsonic aerodynamic requirements, control surface size, and center-of-gravity positions on the initial wing design were investigated.

Nomenclature

R	= aspect ratio
b_{st}	= structural span (exposed wing half chord length), m
\bar{c}	= mean aerodynamic chord, m
c.g.	= center-of-gravity position, x/l_b
C_L	= lift coefficient, lift/ $q_\infty S_{ref}$
C_m	= pitching-moment coefficient, pitching moment/ $q_\infty S_{ref} \bar{c}$
C_{mCL}	= static longitudinal stability based on \bar{c} , $\partial C_m / \partial C_L$
C_p	= local pressure coefficient, $p_L - p_\infty / q_\infty$
$c_{r,exp}$	= exposed root chord, m
K	= Newtonian parameter
l_b	= body length, m
l_{ov}	= wing overhang distance, m
l_{bf}	= body-flap length, m
M	= Mach number
m_L	= vehicle landed mass, kg
Δm_p	= increment in payload mass, kg
m_w	= wing mass, kg
Δm_w	= increment in wing mass, kg
p_L	= local pressure, N/m ²
p_∞	= freestream pressure, N/m ²
q_∞	= freestream dynamic pressure, N/m ²
S_{elevon}	= elevon area, m ²
S_{exp}	= exposed wing area, m ²
S_{ref}	= wing reference area, m ²
t/c	= root thickness-to-chord length ratio
x	= body station position, m
ULF	= ultimate load factor
V_{des}	= design landing requirements, m/s
α	= angle of attack, deg
α_i	= wing incidence angle, deg
α_{trim}	= hypersonic trim angle of attack, deg
$\alpha_{trim,c}$	= constrained hypersonic trim angle of attack, deg
δ	= panel hypersonic impact angle of attack, deg
δ_e	= elevon deflection angle, deg
λ	= wing taper ratio
Λ_{le}	= wing leading-edge sweep, deg
Λ_{hl}	= elevon hinge-line sweep, deg
Λ_{te}	= wing trailing-edge sweep, deg

Introduction

ADVANCED Earth-orbital transportation systems are being studied to identify potential replacements for the Space Shuttle near the year 2000. By analyzing these potential vehicles now, the critical technology areas essential to their development can be identified and prioritized for future research. Various Earth-orbital transportation systems, ranging from Space Shuttle growth options to completely innovative vehicle designs, have been analyzed. One of these vehicle systems is a single-stage-to-orbit (SSTO) vehicle, which is being used as a focus for identifying critical and high-yield technology areas because of its extreme sensitivity to technological advances.

One SSTO concept currently being studied is a vertical takeoff vehicle using liquid oxygen/liquid hydrogen rocket propulsion. After completing its orbital mission, the vehicle re-enters the atmosphere at hypersonic speeds and lands horizontally. In order to fly this mission profile, a wing-body-tail configuration much like the Space Shuttle Orbiter has evolved. As was shown in Refs. 1 and 2, wing design for the Space Shuttle Orbiter was a complex problem because of various stringent requirements such as a maximum allowable landing speed, acceptable unaugmented low-speed flying qualities, and stable hypersonic trim at high angles of attack. In Refs. 1 and 2, matrices of wing geometries were investigated analytically to find a wing geometry that best met the system requirements. Although both methods were seeking minimum mass wings which met the design requirements, no true analytical optimization techniques were used to determine the optimum wing design.

In the present analysis, a method has been developed to analyze the wing design of an SSTO vehicle using a proven optimization technique. A hypersonic and subsonic aerodynamic computer program was developed and combined with a projected gradient optimization algorithm. This analysis program was then used to size and shape a wing that satisfies hypersonic trim and landing requirements for a minimum mass design. The wing parameters included in the analysis were exposed wing area, taper ratio, and leading- and trailing-edge sweep. With this method, the influence of hypersonic and subsonic aerodynamic requirements, control surface size, and c.g. position on wing design were investigated.

Method of Analysis

Baseline Vehicle Description

A point design for a SSTO vehicle was used as a baseline for developing a method of wing sizing optimization.³ The design requirements for the baseline vehicle are based primarily on

Presented as Paper 82-0174 at the AIAA 20th Aerospace Sciences Meeting, Orlando, Fla., Jan. 11-14, 1982; submitted Jan. 22, 1982; revision received May 13, 1982. This paper is declared a work of the U.S. Government and therefore is in the public domain.

*Aerospace Engineer, Space Systems Division. Member AIAA.

Space Shuttle mission specifications. Although the advanced vehicle might be designed for a different mission than the Shuttle, the Shuttle design requirements provide a convenient means for comparing the performance potential of advanced systems.

For the SSTO concept, a 20-yr advancement in both structural and propulsion technology beyond the Space Shuttle level has been assumed. A 25% mass reduction from current structures technology was projected in Ref. 4, basically because of advanced structural concepts and advanced materials. This 25% mass reduction from Shuttle technology has been assumed for the wing, body, tail, propellant tanks, and landing gear. There is no mass reduction assumed for the other subsystems or the thermal protection system. In the area of propulsion, the engine characteristics are based on Space Shuttle main engine technology that has been extrapolated for a two-position nozzle. With a two-position nozzle, a low expansion ratio is used for liftoff to minimize back pressure losses. After the vehicle has reached an altitude near vacuum conditions, the engine nozzles are extended to the higher expansion ratio to increase specific impulse. Since more thrust is available than needed, some of the engines are not equipped with the two-position nozzle and are shut down at this transition point. With the two-position nozzle, the vehicle performance is improved with the trade of increased specific impulse with increased engine mass.⁵

The baseline vehicle was sized for a Shuttle-type payload of 29,500 kg to be carried in a cargo bay 4.6 m in diameter by 18.3 m long to low-Earth orbit. The vehicle is vertically launched from Kennedy Space Center and enters a 92.6×193.2 km orbit inclined at 28.5 deg. The ascent trajectory performance was determined with the program to optimize simulated trajectories.⁶ The trajectory was constrained by a maximum axial acceleration of 3 g's and a maximum normal force of 2.5 times the landed weight of the vehicle, which corresponds to a 2.5 g subsonic pullout maneuver during re-entry.

After the vehicle has completed an orbital mission, it must re-enter the atmosphere at hypersonic speeds and then land horizontally. For the SSTO vehicle, the present design criteria at hypersonic speeds is a stable trim angle of attack from 25 to 50 deg. The landing criterion is a maximum landing speed of 84.9 m/s at a 15-deg angle of attack with static stability.

Based on the above requirements and assumptions, a point design vehicle was generated using the Optimal Design Integration system.⁷ The resulting configuration is presented in Fig. 1. The baseline wing for the SSTO vehicle was based on an optimum wing design study for the Space Shuttle¹ with the wing position moved and wing area sized to meet the aerodynamic criteria of the SSTO vehicle. Details of the wing design are presented in Table 1.

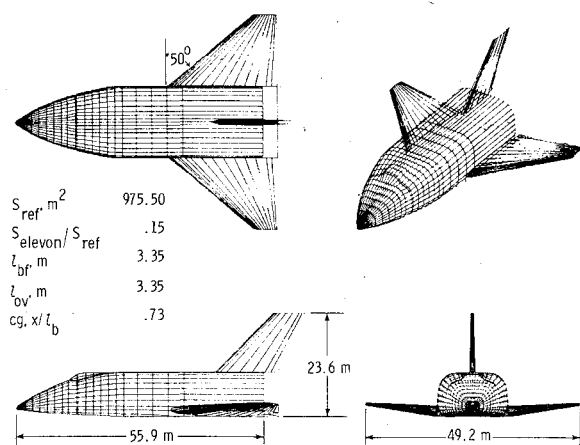


Fig. 1 Baseline vehicle.

Hypersonic Analysis

Since an optimization search technique must evaluate the vehicle's hypersonic trim characteristics many times before the wing mass can be minimized, a rapid hypersonic analysis computer program was developed. Generalized programs that have various options for geometry input and for computing hypersonic aerodynamics, such as that described in Ref. 8, require large computer resources and are unacceptable for rapid optimization studies. The computer program that was developed has the capability of analyzing a wing-body configuration with body-flap and elevon controls approximately 90 times faster than the program described in Ref. 8. In the present method, the body is assumed to consist of a power-law forebody and a constant afterbody (Fig. 2). The forebody is represented by 20 elemental trapezoidal panels. Body camber is represented by a second-order equation which is superimposed on the power law to determine the slope of each individual forebody panel. Both the wing and the body flap are assumed to be flat, quadrilateral panels. The body flap is placed on the body base with a span equal to that of the body. The elevon span is equal to the exposed wing span, and its hinge-line sweep is the same as the trailing-edge sweep.

To calculate the pressure coefficient for each body panel, a modified Newtonian analysis was used:

$$C_p = K \sin^2 \delta \quad (1)$$

As in Ref. 9, the total wing pressure is computed for the entire wing, which includes the undeflected elevon. When the elevon is deflected, the pressure on the elevon at the deflected angle is added to the total wing pressure, and the pressure of the elevon at the slope equal to that of the wing ($\alpha + \alpha_i$) is subtracted. For the condition

$$\alpha + \alpha_i + \delta_e \leq 0 \quad (2)$$

the elevon is assumed to be shadowed from the flow.

Table 1 Baseline wing design

S_{exp} , m ²	487.3
Λ_{le} , deg	50.0
Λ_{te} , deg	0.0
λ	0.15
\mathcal{R}	2.48
b_{sl} , m	19.0
$c_{r,exp}$, m	24.6
m_w , kg	22596.0
c.g., x/l_b	0.70

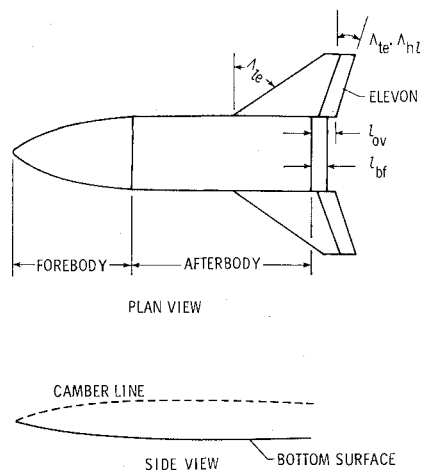


Fig. 2 Hypersonic analysis model.

Corrections were applied to the basic analytical program because of differences between analytical and experimental results. The experimental results were obtained for a 0.0025-scale SSTO configuration (Fig. 3), which was tested in the 22-in. aerodynamics leg in the Hypersonic Helium Tunnel Facility at $M=20$. Reference 8 suggests varying the Newtonian parameter K for each impact angle in order to reflect experimental results. The value of K was varied from its theoretical value of 2 at each angle of attack for each component—wing, body, body flap, and elevon. As shown in Fig. 4, small variations were applied to K for the body, wing, and body flap, but large variations were needed for the elevon at high angles of attack. Using these modified K values, the resulting comparison of pitching-moment coefficient to experimental results are shown in Fig. 5 for the configuration in Fig. 3. The present method using the adjusted values for K also agreed quite well with experimental pitching-moment data for an early Space Shuttle Orbiter configuration.¹⁰

For the wing design problem, a minimum hypersonic stable trim angle of attack for a given wing geometry was determined. For the trim calculation, maximum elevon and body-flap deflections were restricted to positive (down) values of 10 and 14 deg, respectively. These values were chosen to reflect

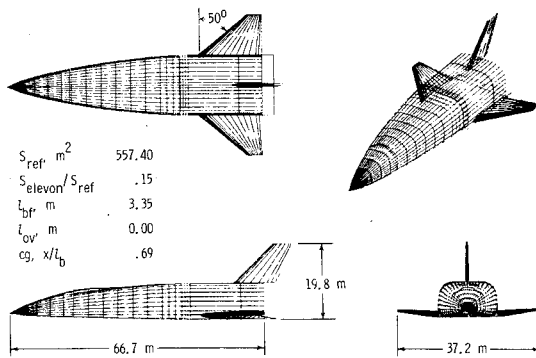


Fig. 3 Experimental model geometric shape (full-scale).

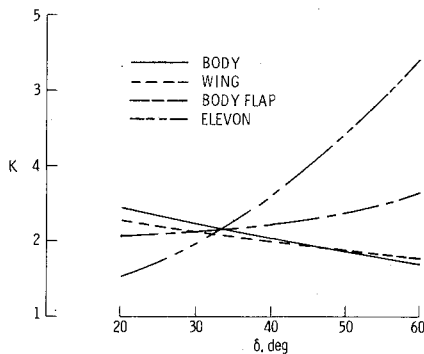


Fig. 4 Experimentally corrected values of the Newtonian parameter applied to vehicle components.

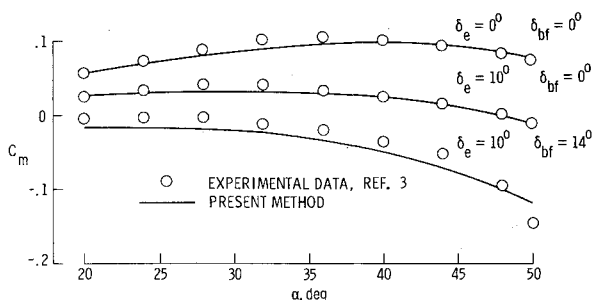


Fig. 5 Theoretical and experimental values of pitching-moment coefficient for the baseline SSTO vehicle at $M=20$.

Space Shuttle Orbiter criteria to limit aerodynamic heating on the control surfaces. The angle of attack for the vehicle was varied from 14 to 60 deg in 2-deg increments. For a fixed body-flap deflection of 14 deg, the elevon deflection was varied from 10 deg down to 40 deg up at 10-deg increments. Stable hypersonic trim angle of attack was determined for each of the elevon deflections, and a minimum trim angle of attack was interpolated.

Subsonic Analysis

The subsonic aerodynamic analysis is based on Datcom methods¹¹ which are empirical equations based on extensive wind tunnel tests. The Datcom manual recommends that these methods be used as increments from experimental values. Thus the subsonic aerodynamics (C_L , C_D , and C_m) computed by the Datcom methods were corrected due to the differences between the prediction results of an SSTO configuration and the experimental results of an 0.01-scale model which was tested in the NASA 7 x 10 low-speed tunnel.³ Data for the body and tail were not changed from the experimental values since they were not perturbed in this study. Tables used in the Datcom methods were programmed as discrete data points, and linear interpolating n -dimensional lookup routines were used to retrieve the correct data from these tables.

In this study, the design landing speed was obtained from the Space Shuttle criteria. The design landing speed is level flight at sea-level angle of attack which has been used for various SSTO studies. To compute the landing speed, vehicle landed mass was held constant at the baseline 204,000 kg.

Wing Mass Estimation

For the design of aerospace vehicles, aerodynamic surfaces are sized to meet a specified aerodynamic performance level at a minimum mass. To minimize wing mass in preliminary design, wing exposed area and structural span are minimized and the root chord thickness is maximized to reduce physical size, bending moment, and internal stresses. Using these three parameters and an ultimate load factor, Ref. 12 establishes a mass estimating relationship based on the wing mass of a number of various aircraft. This relationship has been updated to reflect a 25% mass reduction in wing mass for future vehicles. The wing mass equation used to determine the mass of the exposed wing structure, the carry-through structure, and the thermal protection system (TPS) in kilograms is

$$m_w = (10566) (0.75) \left[\frac{(m_L) (ULF) (b_{st}) (S_{exp})}{10^9 (t/c) (c_{r,exp})} \right]^{0.584} + (7.812) (2.08 S_{exp}) \quad (3)$$

The first term of the equation is the mass of the exposed wing and its carry-through structure. The values 10566, 0.584, and 10^9 are empirical correlation constants. The constant 0.75 refers to a 25% mass reduction from the Shuttle level, which has been assumed for the advanced vehicle. The root thickness, t/c , was held constant at 12%. The ultimate load factor (ULF) was equal to 3.75, which represents a 1.5 safety factor on an established maximum 2.5 g re-entry pullout maneuver. Since the vehicle was not resized for changes in wing mass, the vehicle landed mass, m_L , was equal to that of the baseline vehicle. In this context, all wing mass changes were considered as payload increments. It should be noted that there is no direct correspondence between wing mass change and payload since the vertical tail, some subsystems, and growth depend on wing size. The correlation

$$\Delta m_p = -1.1 \Delta m_w \quad (4)$$

is, however, a close estimate of the payload mass increment and represents the growth change, a constant vertical tail size, and a negligible subsystem mass change.

The second term of Eq. (3) is the mass relationship for the thermal protection system. The term $(2.08 S_{exp})$ is an estimation of the wetted area of the exposed wing. The constant 7.812 is the TPS unit mass which compares to the Space Shuttle Orbiter TPS unit mass of 8.759. Less TPS mass per unit area will be required for an SSTO vehicle because of its lower re-entry planform loading.

It must be noted that the mass equation is used only as a guide for optimizing wing area, structural span, and root-chord length. It is used in this study to estimate the relative effects of geometry wing sizing on wing mass.

Optimization Technique

The optimization technique utilized for the wing design problem is an accelerated projected gradient algorithm (PGA) that is used as the basic optimization technique in the program to optimize simulated trajectories.⁶ The PGA is a combination of Rosen's projection method¹³ and Davidon's method for unconstrained optimization.¹⁴ The PGA solves a general class of nonlinear problems by an iterative technique. Initially, the PGA is a constraint-satisfaction algorithm. After the constraints are satisfied, the algorithm changes to a cost function reduction algorithm if the number of constraints are less than the number of independent variables.

In applying the PGA to the wing size problem, the independent variables were specified as the four basic wing geometry parameters— Λ_{le} , Λ_{te} , λ , and S_{ref} . The constraints were the aerodynamic performance parameters, hypersonic α_{trim} , landing V_{des} , subsonic static margin, and L/D (Table 2). The parameter to be minimized was the wing mass, m_w . The PGA acts as a controller to direct the design process as shown in Fig. 6. The aerodynamic parameters are calculated for the initial values of the wing parameters. Then each of the wing parameters are perturbed, and the changes in the aerodynamic parameters are computed. Using the sensitivities obtained for each of the wing parameters, the program then iterates the parameters until the constraints are satisfied. During this process, active inequality constraints may become inactive if the aerodynamic performance level is satisfied or exceeded. If no constraints become inactive, then there is no optimization, since the number of independent variables equals the number of constraints. If any of the constraints become inactive, then the wing geometry is optimized to reduce the cost function, m_w , while maintaining a satisfactory aerodynamic performance level. A typical optimization problem took approximately 5 minutes on a minicomputer.

Results and Discussion

For various system parameters in the present analysis, wings were sized and shaped to meet both hypersonic and subsonic criteria (Table 2) for a minimum mass. The independent wing geometry variables were λ , Λ_{le} , Λ_{te} , and S_{exp} . The wing position, l_{ov} , was used originally as a parameter, but optimization moved the total wing aft of the body. Thus the position of the wing root chord trailing edge was held constant. All other system parameters were held constant unless they were the subject of analysis. An arbitrary 10-deg trailing-edge sweep maximum bound was used throughout the study to alleviate adverse hypersonic yaw due to roll control that is characteristic of wings with large positive trailing-edge sweep angles.^{2,15}

Center-of-Gravity Position

Single-stage-to-orbit vehicles must include all the propulsion systems needed to achieve orbit. The Space Shuttle is assisted with solid rocket engines which are staged during ascent; thus c.g. position of the SSTO vehicle is understandably further aft than that of the Space Shuttle. A

system study³ determined the c.g. position for the baseline vehicle at 70% l_b as compared to 65-67.5% l_b for the Shuttle. Center-of-gravity ranges for similar SSTO vehicles have been from 68 to 74% l_b .

The wing design for various c.g. positions is presented in Fig. 7 and Table 3. As c.g. moves forward of 0.68 l_b , the exposed area slope decreases and begins to level off because of the V_{des} and L/D constraints as shown in Table 3. For all cases, hypersonic trim, α_{trim} , and static margin were constraints on wing design. Since the number of independent variables was equal to the number of constraints for c.g. positions less than 0.68 l_b , the initial conditions of the independent wing geometry parameters were perturbed manually, as shown in Fig. 6, until a minimum wing mass was determined.

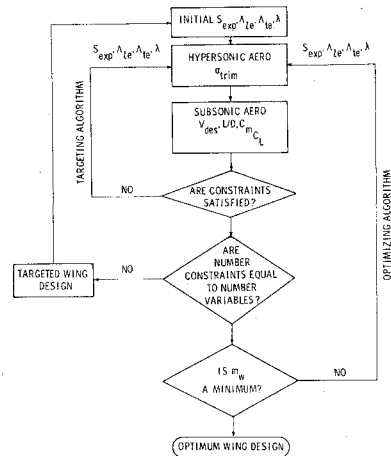


Fig. 6 Wing design procedure.

Table 2 Aerodynamic criteria, wing geometry variables, and system parameters

Aerodynamic criteria	
Hypersonic:	
25 deg $\leq \alpha_{trim} \leq$ 50 deg	
(δ_e between 10 and -40 deg)	
Subsonic:	
$C_m C_L \leq 0.0$	
$L/D \geq 4.5$	
$V_{des} \leq 84.9$ m/s	
Wing geometry variables	
S_{exp}	
Λ_{le}	
Λ_{te} (constrained to 10 deg sweepback)	
System parameters	
c.g., $x/l_b = 0.70$	
$S_{elevation}/S_{ref} = 0.15$	
$l_{bf} = 3.35$ m	

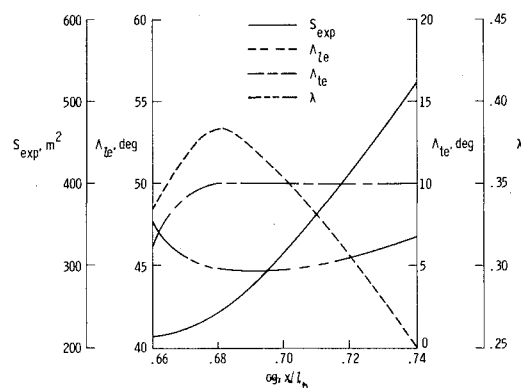


Fig. 7 Effect of center-of-gravity position in wing sizing, $\Lambda_{te,max} = 10$ deg.

For the baseline vehicle, the wing shape was based on an optimum geometry for the Space Shuttle Orbiter in Ref. 1. The exposed area and the wing position were perturbed in order to satisfy the aerodynamic constraints for the baseline SSTO vehicle. By comparing the baseline wing (Fig. 1 and Table 1) to the optimum wing determined in this study for a $0.70 l_b$ c.g. position (Table 4), the wing area was reduced by 30% and the wing mass was reduced by 26%.

Trailing-Edge Sweep

The trailing-edge sweep constraint was changed from 10 to 20 deg (Fig. 8 and Table 4). For c.g. positions greater than $0.69 l_b$, the wing sized to trailing-edge sweeps greater than 10 deg and wing mass is reduced (Fig. 9). Thus for c.g. positions greater than $0.69 l_b$ (beginning range for SSTO vehicles), the trailing edge tends to sweep rearward to minimize wing size. Although there is a benefit in sweeping the trailing edge rearward, there are some constraints to consider, which include the adverse yaw due to roll control, wing scrap angle at touchdown (dictates landing gear length), and rocket plume impingement on the top surface of the wing during launch.

If the wing trailing edge can be swept to 20 deg, then wing mass can be reduced by 28% and wing area by 40% as compared to the baseline wing.

Static Margin Constraint

The subsonic static margin constraint was varied from -0.02 to 0.05 (Fig. 10), which had little effect on wing sizing. Thus for SSTO vehicles with c.g. positions greater than $0.70 l_b$, the dominating aerodynamic design constraint is hypersonic trim, as shown in Table 3.

Hypersonic Criterion

A minimum stable hypersonic trim angle-of-attack criterion has been assumed to be 25 deg. Figure 11 illustrates that wing

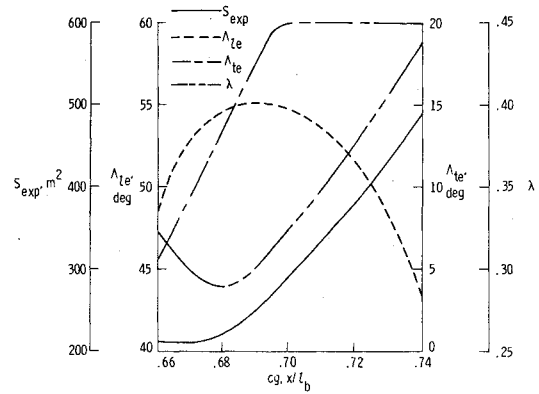


Fig. 8 Effect of center-of-gravity position of wing sizing, $\Lambda_{te,max} = 20$ deg.

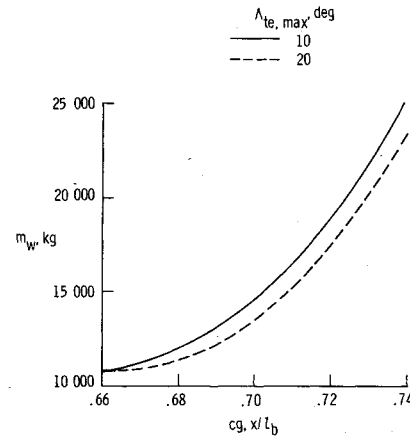


Fig. 9 Effect of trailing-edge sweep constraint on wing sizing.

Table 3 Effect of center of gravity on wing sizing ($\Lambda_{te,max} = 10$ deg)

c.g., x/l_b	0.66	0.68	0.70	0.72	0.74
S_{exp}, m^2	213	247	304	408	526
Λ_{te}, deg	48	53	50	46	40
Λ_{te}^*, deg	5	10*	10*	10*	10*
λ	0.23	0.20	0.20	0.21	0.22
R	1.92	1.84	2.15	2.73	3.40
b_{st}, m	11.7	13.4	15.5	18.9	23.7
$c_{r,exp}, m$	15.6	17.8	18.4	19.8	19.4
m_w, kg	12372	13751	16679	21625	28636
α_{trim}, deg	25†	25†	25†	25†	25†
C_{mCL}	0†	0†	0†	0†	0†
L/D	4.5*	4.7	5.2	5.7	6.4
$V_{des}, m/s$	84.9†	79.7	71.0	67.7	61.4

*Geometric constraint (inactive independent variable).

†Active aerodynamic constraint.

Table 4 Effect of center of gravity on wing sizing ($\Lambda_{te,max} = 20$ deg)

c.g., x/l_b	0.66	0.68	0.70	0.72	0.74
S_{exp}, m^2	213	219	291	381	490
Λ_{te}, deg	48	55	55	52	44
Λ_{te}^*, deg	5	13	20*	20*	20*
λ	0.23	0.19	0.22	0.28	0.34
R	1.92	1.84	1.93	2.00	2.71
b_{st}, m	11.7	13.0	15.9	20.0	21.8
$c_{r,exp}, m$	15.6	16.8	18.6	17.8	18.9
m_w, kg	12372	12782	16270	21587	26601
α_{trim}, deg	25†	25†	25†	25†	25†
C_{mCL}	0†	0†	0†	0†	0†
L/D	4.5†	4.5†	4.7	5.3	5.7
$V_{des}, m/s$	84.9†	84.9†	80.2	73.4	67.7

*Geometric constraint (inactive independent variable).

†Active aerodynamic constraint.

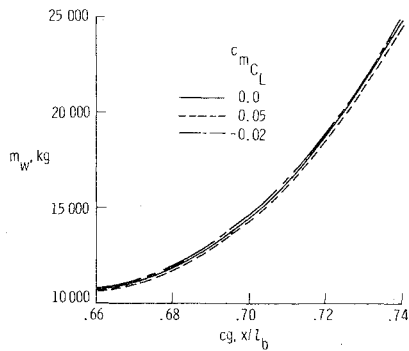


Fig. 10 Effect of static margin constraint on wing sizing ($\Lambda_{te,max} = 10$ deg).

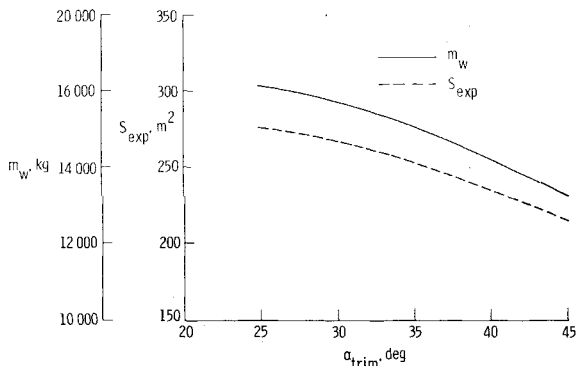


Fig. 11 Effect of hypersonic trim angle-of-attack constraint on wing sizing ($x/l_b = 0.70$, $\Lambda_{te,max} = 10$ deg).

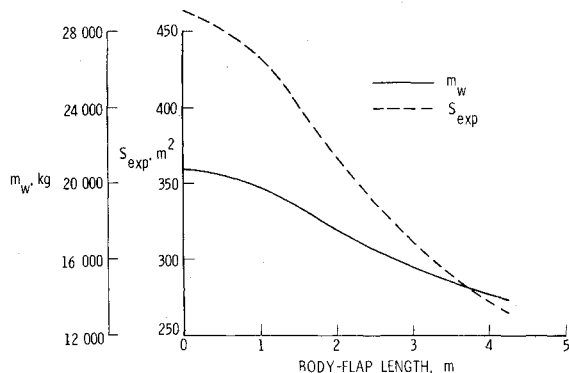


Fig. 12 Body flap length effects on wing sizing ($x/l_b = 0.70$, $\Lambda_{te,max} = 10$ deg).

mass can be decreased by increasing hypersonic trim angle of attack. Thus, re-entry trajectories for an SSTO vehicle need to be investigated in order to maximize the required trim angle of attack, but still meet a cross-range requirement. These investigations would complement re-entry heating investigations, since both would try to maximize the re-entry angle of attack.

Control Surfaces

The body flap for the baseline SSTO vehicle is used for protecting the engine nozzles against aerodynamic heating during re-entry. The body flap can also be used as an effective control surface in the hypersonic speed regime. As shown in Fig. 12, the body flap can significantly reduce the required wing size for hypersonic trim capability; however, like the trailing-edge sweep, the body-flap length is restricted by the impingement of the rocket exhaust plume.

Figure 13 shows the effect of elevon size on wing size. These results indicate that increasing the elevon area by 33% reduces

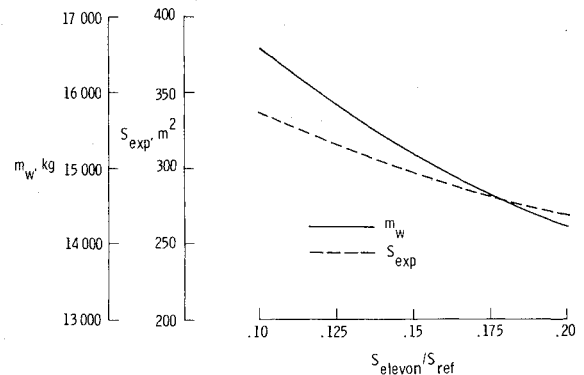


Fig. 13 Effect of elevon size on wing sizing ($x/l_b = 0.70$, $\Lambda_{te,max} = 10$ deg).

wing mass by 5.5%. This reduction in wing mass neglects the increase in system mass that would result with the increase in elevon hinge-line moment that would increase hydraulic actuator requirements.

Concluding Remarks

An investigation has been conducted to determine preliminary wing designs for a single-stage-to-orbit vehicle. Since these vehicles have similar re-entry trajectories to the Space Shuttle Orbiter, the wings were sized to meet Shuttle criteria for hypersonic trim and design landing conditions. A hypersonic and subsonic aerodynamic computer program was developed and combined with an existing optimization algorithm. This combination of computer programs facilitated wing sizing, since the optimization algorithms sought the correct wing geometry that satisfied all aerodynamic criteria for a minimum wing mass design.

Using this method, wings were designed for a range of c.g. positions. Wing size dramatically increases for c.g. positions greater than $0.68 l_b$. The wing sized for the baseline c.g. position ($0.70 l_b$) showed a 26% reduction in wing mass and a 38% reduction in wing area from the baseline wing design, which was based on optimum wing geometry for one Space Shuttle Orbiter design. By changing the trailing-edge sweep constraint from 10 to 20 deg, wing size was further reduced.

Varying the static margin constraint had little effect on wing size, but increasing the hypersonic trim angle of attack had a significant effect in reducing wing size. The landing constraints had no effect until the c.g. position was forward of $0.69 l_b$. Thus, for preliminary wing design, the hypersonic criteria are the most dominant constraints in wing sizing for SSTO vehicles with c.g. positions aft of $0.69 l_b$.

References

- Phillips, W.P., Decker, J.P., Rau, T.R., and Glatt, C.R., "Computer-Aided Space Shuttle Orbiter Wing Design Study," NASA TN D-7478, 1974.
- Surber, T.E., Bornemann, W.E., and Miller, W.D., "Wing Optimization for Space Shuttle Orbiter Vehicles," Space Shuttle Aerothermodynamics Technology Conference, NASA TM X-2508, 1972, pp. 831-859.
- Freeman, D.C. and Wilhite, A.W., "Effects of Relaxed Static Stability on a Single-Stage-to-Orbit Vehicle Design," NASA TP 1594, 1979.
- Brooks, G.W., "Developing Structures Technology for the Day After Tomorrow," *Astronautics and Aeronautics*, Vol. II, July 1973, pp. 56-66.
- Eldred, C.H., Rehder, J.J., and Wilhite, A.W., "Nozzle Selection for Optimized Single-Stage Shuttles," IAF-76-162, 1976.
- Bauer, G.L., Cornick, D.E., Habeger, A.R., Peterson, F.M., and Stevenson, R., "Program to Optimize Simulated Trajectories (POST)," NASA CR-132689, 1975.
- Glatt, C.R. and Hague, D.S., "ODIN: Optimal Design Integration System," NASA CR-2492, 1975.

⁸Gentry, A.E. and Smyth, D.N., "Hypersonic Arbitrary-Body Aerodynamic Computer Program (Mark III Version)," Rept. DAC 61552 (Air Force Contract Nos. F33615 67 C 1008 and F 33615 67 C 1602), McDonnell Douglas Corp., Vol. I, April 1968.

⁹Truitt, R.W., *Hypersonic Aerodynamics*, The Ronald Press Co., 1959, pp. 335-338.

¹⁰Rainey, R.W., Ware, G.M., Powell, R.W., Brown, L.W., and Stone, D.R., "Grumman H-33 Space Shuttle Orbiter Aerodynamic and Handling-Qualities Study," NASA TN D-6948, 1972.

¹¹Hoak, A.F. and Ellison, D.E., "USAF Stability and Control DATCOM," McDonnell Douglas Corp., and U.S. Air Force, Sept. 1970.

¹²Glatt, C.R., "WAATS—A Computer Program for Weights Analysis of Advanced Transportation Systems," NASA CR-2420, 1974.

¹³Rosen, J.B., "The Gradient Projection Method for Nonlinear Programming. Part I—Linear Constraints and Part II—Nonlinear Constraints," *J. Soc. Ind. Appl. Math.*, No. 8, 1961.

¹⁴Davidon, W.C., "Variable Metric Method for Minimization," Rept. AWL-5990 (Rev.), Argonne National Laboratory, Oak Park, Ill., 1959.

¹⁵Arrington, J.P. and Ashby, G.E., "Effect of Configuration Modifications on the Hypersonic Aerodynamic Characteristics of a Blended Delta Wing Body Entry Vehicle," NASA TM X-2611, 1972.

From the AIAA Progress in Astronautics and Aeronautics Series . . .

AEROTHERMODYNAMICS AND PLANETARY ENTRY—v. 77 HEAT TRANSFER AND THERMAL CONTROL—v. 78

Edited by A. L. Crosbie, University of Missouri-Rolla

The success of a flight into space rests on the success of the vehicle designer in maintaining a proper degree of thermal balance within the vehicle or thermal protection of the outer structure of the vehicle, as it encounters various remote and hostile environments. This thermal requirement applies to Earth-satellites, planetary spacecraft, entry vehicles, rocket nose cones, and in a very spectacular way, to the U.S. Space Shuttle, with its thermal protection system of tens of thousands of tiles fastened to its vulnerable external surfaces. Although the relevant technology might simply be called heat-transfer engineering, the advanced (and still advancing) character of the problems that have to be solved and the consequent need to resort to basic physics and basic fluid mechanics have prompted the practitioners of the field to call it thermophysics. It is the expectation of the editors and the authors of these volumes that the various sections therefore will be of interest to physicists, materials specialists, fluid dynamicists, and spacecraft engineers, as well as to heat-transfer engineers. Volume 77 is devoted to three main topics, Aerothermodynamics, Thermal Protection, and Planetary Entry. Volume 78 is devoted to Radiation Heat Transfer, Conduction Heat Transfer, Heat Pipes, and Thermal Control. In a broad sense, the former volume deals with the external situation between the spacecraft and its environment, whereas the latter volume deals mainly with the thermal processes occurring within the spacecraft that affect its temperature distribution. Both volumes bring forth new information and new theoretical treatments not previously published in book or journal literature.

Volume 77—444 pp., 6 × 9, illus., \$30.00 Mem., \$45.00 List

Volume 78—538 pp., 6 × 9, illus., \$30.00 Mem., \$45.00 List

TO ORDER WRITE: Publications Dept., AIAA, 1290 Avenue of the Americas, New York, N.Y. 10104